Molecular Biology of the Cell
Vol. 15, 5516–5527, December 2004

p116^{Rip} Targets Myosin Phosphatase to the Actin Cytoskeleton and Is Essential for RhoA/ROCK-regulated Neuritogenesis

Jacqueline Mulder, Aafke Ariaens, Dick van den Boomen, and Wouter H. Moolenaar*

Division of Cellular Biochemistry and Centre for Biomedical Genetics, The Netherlands Cancer Institute, 1066 CX Amsterdam, The Netherlands

Submitted April 1, 2004; Revised September 17, 2004; Accepted September 23, 2004
Monitoring Editor: Anne Ridley

Activation of the RhoA–Rho kinase (ROCK) pathway stimulates actomyosin-driven contractility in many cell systems, largely through ROCK-mediated inhibition of myosin II light chain phosphatase. In neuronal cells, the RhoA–ROCK–actomyosin pathway signals cell rounding, growth cone collapse, and neurite retraction; conversely, inhibition of RhoA/ROCK promotes cell spreading and neurite outgrowth. The actin-binding protein p116^{Rip}, whose N-terminal region bundles F-actin in vitro, has been implicated in Rho-dependent neurite remodeling; however, its function is largely unknown. Here, we show that p116^{Rip}, through its C-terminal coiled-coil domain, interacts directly with the C-terminal leucine zipper of the regulatory myosin-binding subunits of myosin II phosphatase, MBS85 and MBS130. RNA interference-induced knockdown of p116^{Rip} inhibits cell spreading and neurite outgrowth in response to extracellular cues, without interfering with the regulation of myosin light chain phosphorylation. We conclude that p116^{Rip} is essential for neurite outgrowth and may act as a scaffold to target the myosin phosphatase complex to the actin cytoskeleton.

INTRODUCTION

Small GTP-binding proteins of the Rho family, notably, RhoA, Rac, and Cdc42, are key regulators of the actin cytoskeleton in response to extracellular cues (Etienne-Manneville and Hall, 2002). In particular, RhoA regulates actomyosin-driven contractile events and morphological changes in many cell types, including those of the nervous system (Hall, 1998; Kaibuchi *et al*., 1999; Luo, 2000). It does so primarily by stimulating the activity of Rho-kinase (ROCK), which phosphorylates the regulatory myosin-binding subunit (MBS) of myosin light chain (MLC) phosphatase. When phosphorylated by ROCK, MBS inhibits the activity of MLC phosphatase and thereby promotes MLC phosphorylation and actomyosin contractility (Kimura *et al*., 1996; Kawano *et al*., 1999). In neuronal cells, activation of the RhoA–ROCK–actomoysin pathway is necessary and sufficient to induce growth cone collapse, retraction of developing neurites, and transient rounding of the cell body in response to certain receptor agonists, such as lysophosphatidic acid (LPA), thrombin, and sphingosine-1-phosphate (Jalink *et al*., 1994; Postma *et al*., 1996; Kozma *et al*., 1997; Amano *et al*., 1998; Hirose *et al*., 1998; Bito *et al*., 2000). Conversely, inactivation of the RhoA–ROCK pathway, by using pharmacological inhibitors or dominant-negative constructs, is sufficient to promote neurite outgrowth and growth cone motility (Jalink *et al*., 1994; Kozma *et al*., 1997; Hirose *et al*., 1998; Bito *et al*., 2000). From these studies, it has emerged that RhoA–actin pathways are fundamental to neurite remodeling, guidance, and branching not only in neuronal cell lines but also in primary neurons (Luo, 2000, 2002). Many questions remain, however, because it still unclear how components of Rho signaling pathways are compartmentalized and assembled into functional signaling modules, and how the specificity of signal transduction is controlled.

Various actin-associated proteins participate in regulating cytoskeletal dynamics downstream of Rho GTPases, with some proteins arranging actin into higher order structures and others controlling actin remodeling in response to physiological stimuli (Ayscough, 1998; Bamburg, 1999; Borisy and Svitkina, 2000; Wear *et al*., 2000; Higgs and Pollard, 2001; Da Silva *et al*., 2003). We previously identified a ubiquitously expressed protein of predicted size 116 kDa, named p116^{Rip}, that binds relatively weakly to constitutively active RhoA(V14) in a yeast two-hybrid assay (Gebbink *et al*., 1997). The p116^{Rip} sequence reveals several protein interaction domains, including two pleckstrin homology domains, two proline-rich stretches, and a C-terminal coiled-coil domain; it lacks any known catalytic motif. When overexpressed in N1E-115 neuroblastoma cells, p116^{Rip} promotes cell flattening and neurite extension and inhibits LPA-induced neurite retraction, reminiscent of what is observed after RhoA inactivation by using dominant-negative RhoA or the Rho-inactivating C3 toxin (Gebbink *et al*., 1997). This led us to hypothesize that p116^{Rip} may negatively regulate RhoA signaling. More recently, however, we found that p116^{Rip}, rather than directly binding to RhoA (Gebbink *et al*., 2001), interacts through its N-terminal region with F-actin and colocalizes with dynamic actomyosin-rich structures, including stress fibers and cortical microfilaments in filopodia and lamellipodia (Mulder *et al*., 2003). Furthermore, we

Article published online ahead of print. Mol. Biol. Cell 10.1091/mbc.E04–04–0275. Article and publication date are available at www.molbiolcell.org/cgi/doi/10.1091/mbc.E04–04–0275.

* Corresponding author. E-mail address: w.moolenaar@nki.nl.

found that p116Rip induces bundling of F-actin in vitro, with the bundling activity residing in the N-terminal region. Despite being an actin-bundling protein, overexpression of p116Rip or its N-terminal actin-binding domain in neuroblastoma cells disrupts the actin cytoskeleton and thereby inhibits actomyosin contractility to promote neurite outgrowth (Mulder *et al*., 2003). Thus, p116Rip is an actin-binding protein that may act as a scaffold for multiple protein interactions involved in neurite remodeling.

To understand the normal biological function of p116Rip in neuritogenesis, we set out to identify binding partners of the C-terminal domain of p116Rip and to undertake a loss-of-function analysis by using RNA interference (RNAi). We report here that the coiled-coil domain of p116Rip interacts directly with the regulatory myosin-binding subunits of MLC phosphatase, MBS85 and MBS130. Furthermore, our RNAi studies show that p116Rip-deficient cells fail to undergo neurite outgrowth in response to various extracellular cues (RhoA/ROCK inhibition, intracellular cAMP elevation, or growth factor deprivation), whereas the regulation of MLC phosphorylation remains intact. Thus, p116Rip is an essential component in the RhoA/ROCK–actomyosin pathway that regulates neuritogenesis.

MATERIALS AND METHODS

Cell Culture, Transfection, and Materials

All cells were cultured in DMEM containing 8% fetal calf serum. Human Embryonic kidney (HEK)293 cells were transfected using calcium phosphate precipitation. N1E-115 and Neuro-2A cells were transfected using FuGENE 6 reagent (Roche Diagnostics, Mannheim, Germany) according to the manufacturer's protocol. COS-7 cells were transfected using DEAE–dextran as described previously (Zondag *et al*., 1996). The following materials were obtained from the designated sources: dibutyryl-cAMP (db-cAMP) (Sigma-Aldrich, St. Louis, MO), calyculin A (CA) and Y-27632 (Calbiochem, San Diego, CA), 1-oleoyl-LPA (Sigma-Aldrich), FLAG M2 mouse monoclonal antibody (mAb) (Sigma-Aldrich), rabbit anti-PP1δ and anti-cortactin 4F11 (Upstate Biotechnology, Lake Placid, NY), anti-actin mAb (Chemicon International, Temecula, CA), rabbit anti-green fluorescent protein (GFP) (van Ham *et al*., 1997), anti-phospho-MLC-Thr18/Ser19 (Cell Signaling Technology, Beverly, MA), anti-myc 9E10 mAb and anti-HA 12CA5 mAb from hybridoma supernatants (American Type Culture Collection, Manassas, VA), and anti-MBS130 (CRP, Berkely, CA). Rabbit p116Rip antibodies directed against glutathione *S*-transferase-Rho-binding domain (GST-RBD) (amino acids 545–823) have been described previously (Gebbink *et al*., 1997). Rabbit anti-p116Rip serum (p116RipNT) directed against the N terminus of p116Rip (amino acids 1–382) was made by immunizing rabbits with purified GST-N-terminal (NT) protein (Mulder *et al*., 2003). p116RipNT antibodies were used to immunoprecipitate p116Rip from N1E-115 lysates because p116Rip antibodies directed against RBD compete with MBS for the same binding site on p116Rip.

RNAi and Plasmids

The p116Rip RNAi targeting vectors (pS-GFPp116Rip) were based on a 19-mer sequence present in the coding sequence of human, rat, and mouse p116Rip: 5′-gagcaagtgtcagaactgc-3′. 64-mer synthetic oligonucleotides for cloning into pSuperGFP (pS-GFP) were synthesized, annealed, and ligated into the pS-GFP plasmid or into the pS plasmid as described previously (Brummelkamp *et al*., 2002a). To obtain retroviral pSuper constructs (pRS), pS-p116Rip was digested with *EcoR*I-*Xho*I and the insert containing the RNAi targeting sequence and promotor was ligated into pRS (Brummelkamp *et al*., 2002b). The pS-GFP plasmid consists of the pS plasmid including the GFP protein under control of a pGK promoter. Adenoviral pAS constructs were designed as follows: pS-p116Rip or pS were digested with *Xho*I-*Bam*HI and the insert containing the RNAi targeting sequence and promotor was ligated into pENTR1A of the virapower adenoviral expression system (Invitrogen, Carlsbad, CA). The p116Rip point mutants (L857P, L905P, and I919P) were obtained using the QuikChange site-directed mutagenesis kit (Stratagene, La Jolla, CA) by using pcDNA3-HA-FLp116Rip (Mulder *et al*., 2003) as a template. pcDNA3-HA-ΔNp116Rip was generated from Mb2a-p116Rip-ΔN; pcDNA3-HA-NTp116Rip, pcDNA3-HA-CTp116Rip, and pcDNA3-HA-RBDp116Rip have been described previously (Gebbink *et al*., 1997; Mulder *et al*., 2003); pcDNA3-HA-FLp190RhoGEF and pcDNA3-HA-Coil-p190RhoGEF are described by van Horck *et al*. (2001). pXJ40-FLAG-p85 (MBS) and pEFBOS-myc-MBS130 plasmids were kindly provided by Dr. T. Leung (Institute of Molecular and Cell Biology, Singapore) and Dr. K. Kaibuchi (Nagoya University, Nagoya, Japan), respectively.

Yeast Two-Hybrid Analysis

Mb2a-p116Rip-ΔN, in which p116Rip lacking the N terminus is fused to the GAL4 DNA-binding domain of Mb2a, was generated by polymerase chain reaction (PCR) by using primers 5′-acgcgtcgacccggtaccactccacagaatcctccatga-3′ (forward) and 5′-ataagaatgcggccgcaagctttcagttatcccatgagacctg-3′ (reverse). The PCR product was digested with *Sal*I-*Not*I and ligated into Mb2a. Mb2a-p116Rip-ΔN was integrated into the genome of yeast strain Y190 and used as bait in screening a human testis cDNA library in pVP16, according to previously described procedures (Gebbink *et al*., 1997). Binding specificity of cDNAs obtained from positive yeast colonies was confirmed by retransformation assays.

Western Blotting and Immunoprecipitation

COS-7 cells coexpressing various constructs were scraped in ice-cold lysis buffer (1% NP-40, 50 mM Tris, pH 7.4, 200 mM NaCl, 2.5 mM $MgCl_2$, 10% glycerol, supplemented with protease inhibitors). Extracts were clarified by centrifugation and precleared with 0.5% bovine serum albumin (BSA)-blocked protein A-Sepharose beads for 1 h at 4°C. Precleared lysates were incubated overnight with anti-hemagglutinin (HA) at 4°C, and immunocomplexes were removed by incubation with protein A-Sepharose beads for 30 min at 4°C. Beads were washed, resuspended in Laemmli sample buffer, and boiled. Samples were separated by SDS-PAGE and analyzed by Western blotting by using anti-myc, anti-HA, or anti-FLAG antibodies. N1E-115 lysates were prepared similarly, and supernatants were precleared with 0.5% BSA-blocked protein A-Sepharose beads precoupled to either preimmune rabbit serum (IgG), p116RipAB, PP1δ, or anti-MBS antibodies overnight at 4°C. Beads were washed, resuspended in Laemmli sample buffer, and boiled. Samples were separated by SDS-PAGE and analyzed by Western blotting by using anti-MBS, anti-p116Rip, or anti-PP1δ antibodies. HEK293 cells were cotransfected (1:1) with plasmids as indicated; 96 h after transfection, cells were lysed as described above. Blots were incubated with anti-HA and/or anti-actin mAbs. Neuro-2A cells were transfected with plasmids and lysed similarly 96 h after transfection. Blots were incubated with rabbit anti-p116Rip, rabbit anti-GFP, and anti-actin mAb. In all cases, Bradford protein assays were performed on the lysates to test for equal loading on SDS-PAGE.

Fluorescence Microscopy

In RNAi studies, Neuro-2A cells were transfected with pS-GFP, pS-GFPp116Rip, or a combination of pS-GFP/pS-GFPp116Rip and pcDNA3-HA-FLp116Rip variants (ratio 1:8). To induce neurite outgrowth, N1E-115 and Neuro-2A cells were either exposed for 48 h to serum-free Neurobasal medium supplemented with B-27 (NB-B27; Invitrogen) containing db-cAMP (1 mM); alternatively, cells were incubated with Y-27632 (10 μM) for 8 h. Fluorescence and corresponding phase-contrast images pictures were taken on a Zeiss Axiovert microscope equipped with a charge-coupled device camera. GFP-positive cells were analyzed for neurite outgrowth, defined as processes longer than one cell body diameter.

Retroviral Infections and Detection of Myosin Light Chain Phosphorylation

Phoenix-Eco package cells were transfected with pRS or pRS-p116Rip. The supernatant containing viral particles was harvested at 48 and 72 h after transfection. For infection of NIH3T3 cells, cells were incubated with 1 ml of viral stock in the presence of 10 μl of Dotap (1 mg/ml; Roche Diagnostics). The following day, cells were washed with phosphate-buffered saline (PBS) and fresh medium was added. Seventy-two hours after infection, NIH3T3 cells were serum starved (0.1% fetal calf serum [FCS]) for 24 h or left in serum-containing media and then stimulated for 10 min with 2.5 μM LPA, 5 min with 0.1 μM CA, or 45 min with 10 μM Y-27632. Cells were washed once with ice-cold PBS and lysed in Laemmli's sample buffer. Cell lysates were subjected to immunoblotting by using anti-phospho-MLC-Thr18/Ser19, rabbit p116Rip antibodies, and anti-actin mAb.

Adenoviral Infections and Solubility Assay

Adenovirus was produced according to the manufacturer's protocol (virapower adenoviral expression system; Invitrogen). N1E-115 cells were infected with either pAS control or pAS-p116Rip virus (by using equal amounts of virus particles per cell). At 72 h after infection, cells were serum starved. The following day, cells were stimulated for 5 min with 2.5 μM LPA or 4 min with 0.1 μM CA. The Triton solubility assay was performed as described previously (Mulder *et al*., 2003). In brief, detergent lysates were centrifuged for 30 min by using an Eppendorf table centrifuge. Equal amounts of pellet and supernatant fractions were subjected to SDS-PAGE. Proteins were detected by immunoblotting by using antibodies against MBS, cortactin, actin, and p116Rip.

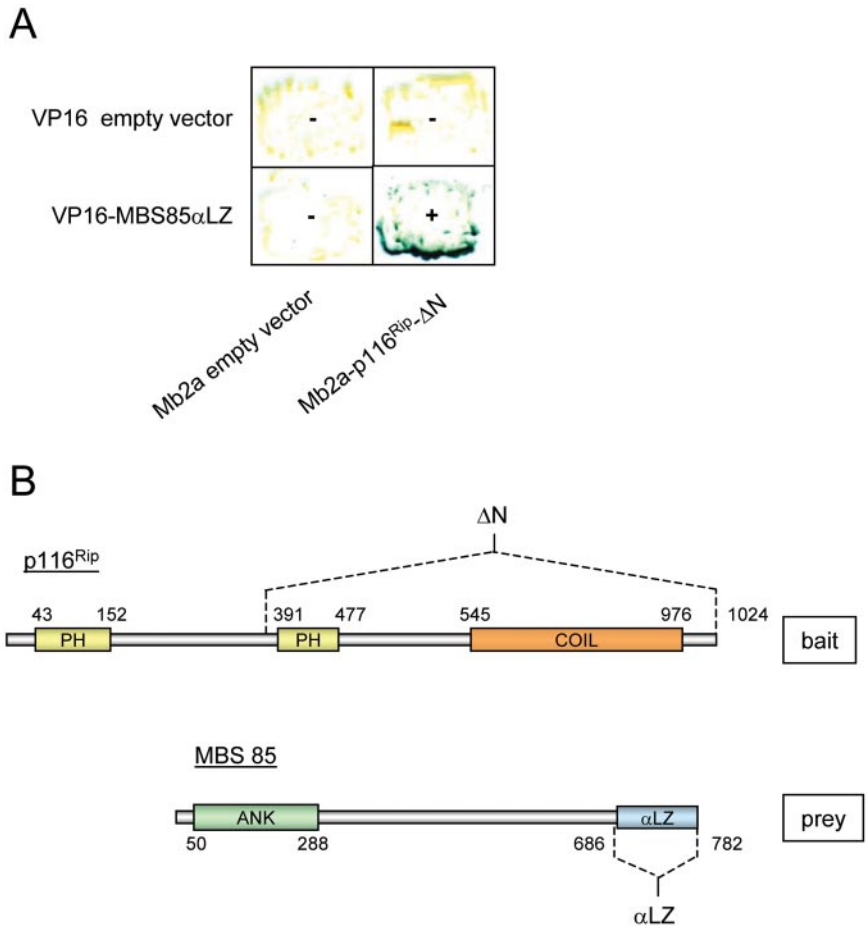

Figure 1. Yeast two-hybrid interaction between p116^{Rip} and MBS85. (A) MBS85 was identified by screening a human testis cDNA library by using the C-terminal part of p116^{Rip} as bait (p116^{Rip}-ΔN). Binding of the α-helical leucine zipper of MBS85 to the C terminus of p116^{Rip} was confirmed in retransformation assays, in which clones became positive for β-galactosidase activity within 1 h. Yeast cells (Y190) were transformed with Mb2a encoding the GAL4 binding domain fused with the C terminus of p116^{Rip} and VP16 encoding the GAL4 activation domain fused with the C terminus of MBS85 and screened for β-galactosidase activity (+). Empty vector controls are indicated. (B) Schematic representation of the interacting domains (bait-prey) in p116^{Rip} and MBS85. PH, pleckstrin homology domain; ANK, ankyrin repeats; Coil, coiled-coil domain; αLZ, α-helical leucine zipper domain. Numbers refer to amino acid residues.

RESULTS

Identification of Myosin Phosphatase Targeting Subunits MBS85 and MBS130 as Binding Partners of p116^{Rip}

We previously reported that the N-terminal region of p116^{Rip} (residues 1–382) binds tightly to F-actin (K_d of ~0.5 μM), shows F-actin-bundling activity in vitro, and dictates the subcellular localization of p116^{Rip} to dynamic actin-rich structures such as stress fibers and cortical microfilaments (Mulder *et al.*, 2003). To identify additional binding partners of p116^{Rip}, we performed a yeast two-hybrid screen with the C-terminal part of p116^{Rip} (aa 391-1024) as bait and a human testis cDNA library as prey. We detected a strong interaction with the very C-terminal leucine-zipper domain (aa 686–782) of the regulatory myosin-binding subunit p85 (MBS85) (Figure 1A). MBS85 is structurally and functionally related to its better-known and more widespread family member MBS130 (Tan *et al.*, 2001), with both proteins containing N-terminal ankyrin repeats and an α-helical leucine zipper at the C terminus. MBS85 is highly expressed in brain and heart, but unlike MBS130, not in smooth muscle (Tan *et al.*, 2001). Through their N-terminal region, MBS85 and MBS130 bind to the catalytic subunit protein phosphatase I (PP1δ; 37 kDa), and thereby regulate phosphatase activity toward the MLC. MBS binds to the active, GTP-bound form of RhoA and is a direct target of ROCK (Kimura *et al.*, 1996). MBS phosphorylation by ROCK results in inhibition of phosphatase activity with a consequent increase in MLC phosphorylation and actomyosin contractility.

A schematic representation of the two-hybrid interaction between the C-terminal parts of p116^{Rip} and MBS85 is shown in Figure 1B. Given the high similarity between MBS85 and MBS130 in their α-helical leucine repeats (66% at the amino acid level) (Tan *et al.*, 2001), we examined the interaction of p116^{Rip} with both MBS85 and MBS130 in COS-7 cells. We found that epitope-tagged forms of MBS85 and MBS130 both coprecipitate with HA-tagged p116^{Rip} (Figure 2, A and B), indicating that the p116^{Rip}-MBS85/130 interaction occurs in vivo.

To map the region in p116^{Rip} that mediates MBS binding, we generated HA-tagged truncation mutants of the C-terminal part of p116^{Rip} and expressed them in COS cells. As a negative control, we used the C-terminal coiled-coil domain of an unrelated protein, the Rho-specific exchange factor p190RhoGEF (van Horck *et al.*, 2001). All p116^{Rip} truncation mutants containing the coiled-coil domain were found to precipitate both MBS130 and MBS85 from COS cell lysates (Figure 2, A–C). No MBS interaction was detected with a truncated coiled-coil mutant (RBD; aa 545–823) or with the isolated N-terminal part of p116^{Rip} (NT; aa 1–382), nor with the coiled-coil domain of p190RhoGEF (Figure 2, A and B). These results indicate that the coiled-coil region of p116^{Rip} (aa 545-1024) interacts specifically with the α-helical leucine zippers of MBS85 and MBS130 and that the MBS-binding region of p116^{Rip} is located within the C-terminal half of the coiled-coil domain (aa 823-1024; Figure 2C).

Leucine zippers are commonly regarded as regular coiled-coil structures (O'Shea *et al.*, 1989), in which the (iso)leucine

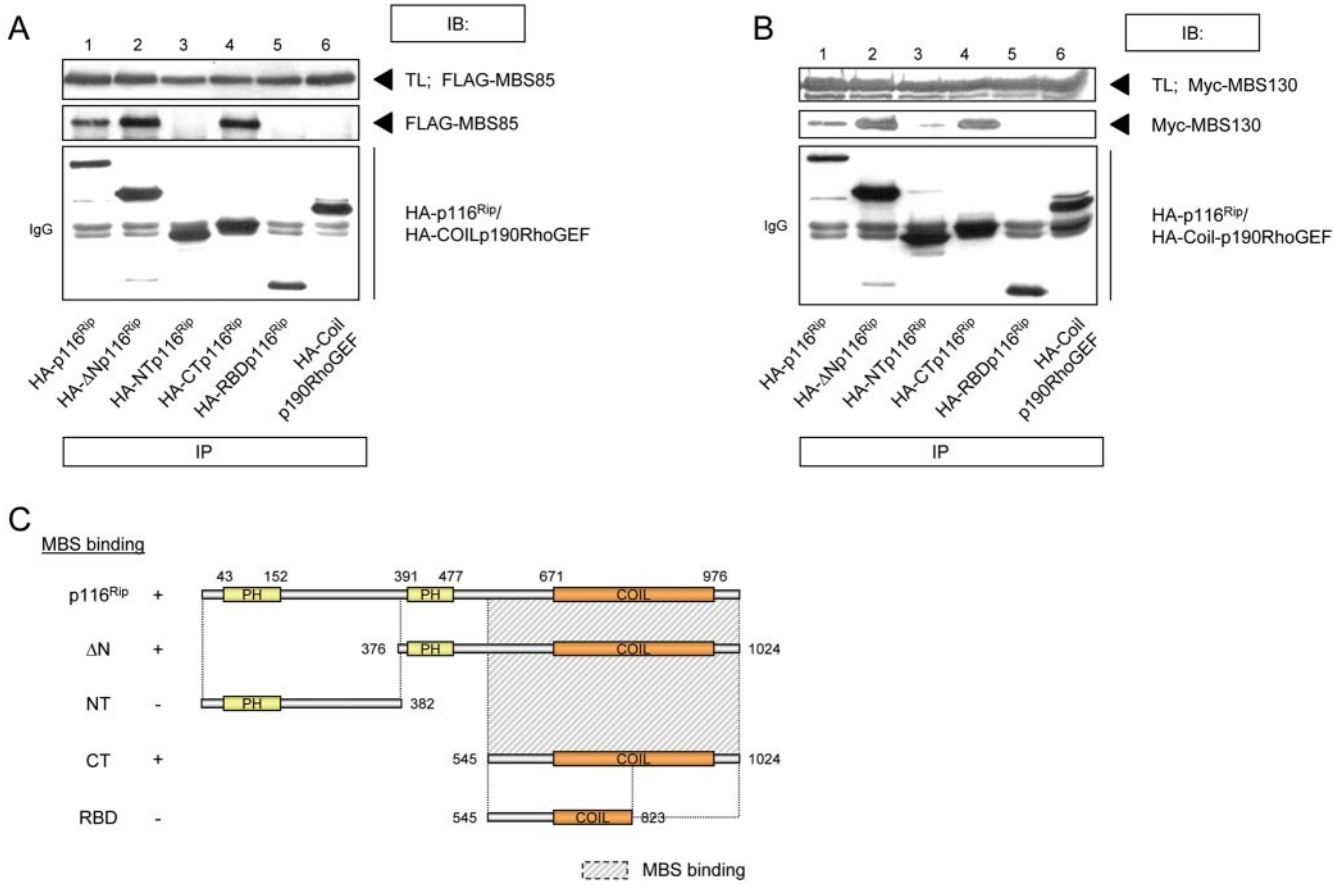

Figure 2. The coiled-coil domain of p116Rip interacts with the C-terminal leucine zipper of MBS85 and MBS130 in mammalian cells. (A and B) COS-7 cells were transfected with plasmids encoding FLAG-MBS85 or Myc-MBS130 and the indicated HA-tagged p116Rip truncation mutants or HA-coil-p190RhoGEF. Total cell lysates (TL) were analyzed for MBS85 and MBS130 expression (top). Immunoprecipitation (IP) of HA-tagged proteins and coprecipitation of MBS85 or MBS130 was analyzed by immunoblotting (IB) by using α-HA, α-FLAG, and α-Myc antibodies. (C) Analysis of the interaction between the coiled-coil domain of p116Rip and the leucine zipper of MBS (MBS85 and MBS130), as determined in COS-7 cells; + denotes interaction with MBS. CT, C-terminal region; RBD, "Rho-binding" domain (as defined in Gebbink *et al.*, 1997).

repeats form a hydrophobic region where side chain interactions mediate protein–protein interaction; mutagenesis of selected (iso)leucine residues (to alanine, valine, or proline) abrogates the interaction (Turner and Tjian, 1989; Hu *et al.*, 1990). To determine whether leucine-isoleucine motifs in the coiled-coil of p116Rip are essential for binding to the MBS leucine zipper, we replaced residues Leu(857), Leu(950), and Ile(919) in p116Rip with Proresidues (Figure 3). Protein–protein interactions were examined by coexpression of these p116Rip mutants with either MBS85 or MBS130. As shown in Figure 3, the L857P and I919P mutants, but not the L905P mutant, failed to interact with MBS85 and MBS130. We conclude that residues Leu(857) and Ile(919) in p116Rip are critical for direct interaction with the leucine-zipper domains of MBS85 and MBS130.

Endogenous Interaction of p116Rip with the Myosin Phosphatase Complex in Neuronal Cells

We next examined complex formation between endogenous p116Rip and MBS130 in neuronal N1E-115 cells. As shown in Figure 4, endogenous MBS130 and p116Rip were coimmunoprecipitated from N1E-115 cell lysates by using a polyclonal anti-p116Rip antibody; endogenous MBS85 could not be detected due to lack of antibodies. Two separate MBS130-reactive bands are observed in p116Rip precipitates from N1E-115 cells (Figure 4A), consistent with MBS130 existing in two isoforms one of which contains a central insertion (Hartshorne, 1998). No MBS130 protein was detected in control immunoprecipitates. MBS associates with the catalytic subunit, PP1δ. Figure 4B shows that p116Rip and MBS130 are both present in PP1δ immunoprecipitates from N1E-115 cells. We conclude that p116Rip is a component of the MBS–PP1δ complex in neuronal cells.

RNAi-induced Knockdown of p116Rip Inhibits Neurite Outgrowth

Transient overexpression of p116Rip results in disassembly of the actin cytoskeleton and promotes neurite extension in N1E-115 cells (Gebbink *et al.*, 1997; Mulder *et al.*, 2003). Expression of the actin-binding region alone (NT-p116Rip) led to the same phenotype, whereas cells expressing the C-terminal domain alone displayed a seemingly normal F-actin pattern (Mulder *et al.*, 2003). Although these results suggest that the N-terminal half of p116Rip is critical for mediating F-actin (dis)assembly, they do not allow any conclusion about the normal physiological function of p116Rip. A more informative and elegant approach to assessing the

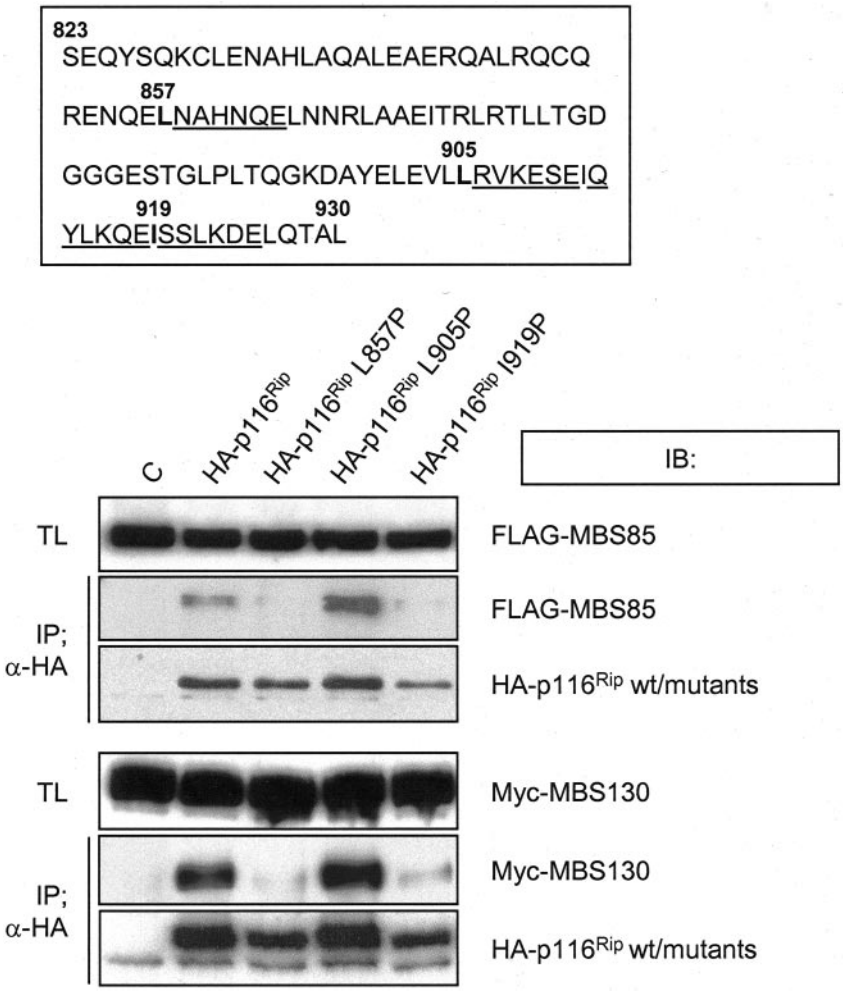

Figure 3. (Iso)leucine residues in the coiled-coil of p116^{Rip} mediate binding to the leucine zippers of MBS85 and MBS130. Representation of residues 823–930 of the coiled-coil domain of p116^{Rip}. Leucine zipper-like motifs are underlined. (Iso)leucines in bold were mutated to proline by site-directed mutagenesis. COS-7 cells were cotransfected with plasmids encoding either FLAG-MBS85 or Myc-MBS130 and indicated HA-tagged plasmids encoding p116^{Rip} (iso)leucine mutants or an empty HA-tagged plasmid as control. Total cell lysates (TL) analyzed for MBS85 and MBS130 expression are shown (top panels in both figures). Immunoprecipitation (IP) of HA-tagged proteins and coprecipitation of MBS85 or MBS130 were analyzed by immunoblotting (IB) by using α-HA, α-FLAG, and α-Myc antibodies.

importance of putative scaffold proteins like p116^{Rip} is to knockdown their endogenous expression levels by RNAi.

We used the expression vector pSUPER, which directs stable expression of small interfering RNAs (Brummelkamp *et al*., 2002a). Persistent suppression of gene expression by this vector allows the analysis of loss-of-function phenotypes that develop over longer periods of time. A GFP-containing construct was created that targets mouse p116^{Rip} mRNA (with GFP expressed from a distinct PGK promotor), termed pSUPER-GFP (pS-GFP). Targeting efficacy was

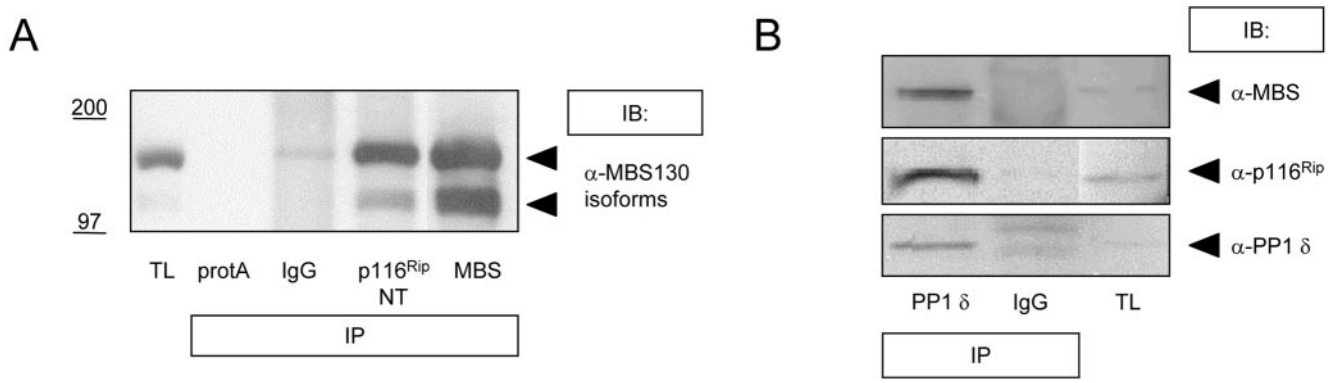

Figure 4. Association of endogenous p116^{Rip} with the MLC phosphatase complex. (A) p116^{Rip} and MBS130 were immunoprecipitated (IP) from N1E-115 cells and subjected to Western blotting (IB) by using MBS130 antibodies. Control lysates were incubated with protein A-Sepharose 4B beads alone or together with control IgG. Both isoforms of MBS130 are detected in p116^{Rip} immunoprecipitates. TL, total cell lysates. (B) PP1δ immunoprecipitates (IP) from N1E-115 cells and TL were subjected to IB by using MBS130, p116^{Rip}, and PP1δ antibodies. MBS130 and p116^{Rip} are seen to coimmunoprecipitate with endogenous PP1δ.

tested in HEK293 cells by cotransfecting HA-p116Rip and pS-GFPp116Rip. HA-p190RhoGEF was used as a negative control (van Horck *et al*., 2001). At 4 d after transfection, HA-p116Rip expression is knocked down by almost 100%, whereas HA-p190RhoGEF expression remains unaffected (Figure 5A). The RNAi construct was then transfected into Neuro-2A and N1E-115 cells to study the phenotypic consequences of p116Rip knockdown. Immunoblot analysis confirmed effective knockdown of endogenous p116Rip in Neuro-2A cells (Figure 5F).

Neurite outgrowth (with concomitant growth arrest) can be induced by various treatments, including pharmacological inhibition of the RhoA-ROCK pathway, elevation of intracellular cAMP levels, and growth factor deprivation. Although control Neuro-2A and N1E-115 cells underwent flattening and neuritogenesis within a few hours after serum withdrawal, we consistently observed that their p116Rip-deficient counterparts (pS-GFP-p116Rip-positive) maintained a rounded shape even after prolonged periods (>48 h) of serum starvation. Also, after prolonged incubation with the membrane-permeable cAMP analogue db-cAMP (4 d), the p116Rip-deficient cells (pS-GFPp116Rip-positive) remain rounded with little or no sign of process extensions: <9% of the p116Rip-depleted cells are capable of sending out neurites compared with 54% of the GFP-expressing control cells (Figure 5, B and C). Finally, addition of the ROCK inhibitor Y-27632 resulted in rapid cell flattening and initiation of neurite outgrowth in both Neuro-2A and N1E-115 cells, whereas the p116Rip-deficient cells failed to show any morphological response to Y-27632 (Figure 5, D and E). Similar results were obtained with the Rho-inactivating C3-exoenzyme (our unpublished data). Coexpression of RNAi-resistant p116Rip (containing three silent mutations in the target sequence) with pS-GFPp116Rip largely restored the morphological responses (our unpublished data), consistent with the observed effects being specific for p116Rip loss-of-function (although introduction of RNAi-resistant p116Rip is in fact "overexpression").

Together, these results indicate that p116Rip is essential for Neuro-2A and N1E-115 cells to send out neurites in response to various extracellular cues, notably, RhoA/ROCK inhibition, growth factor withdrawal, and intracellular cAMP elevation.

p116Rip Deficiency Does Not Impair the Regulation of MLC Phosphorylation

Our observation that p116Rip deficiency interferes with neuritogenesis is reminiscent of what is observed after constitutive activation of the RhoA–ROCK pathway, eventually leading to phosphorylation of the 20-kDa MLC. We therefore examined whether p116Rip deficiency affects the regulation of MLC phosphorylation. Phosphorylation of nonmuscle myosin II on MLC residue Ser-19 regulates both its motor activity and filament assembly (for review, see Bresnick, 1999). MLC phophorylation is mediated mainly by myosin light chain kinase with probably an additional but less established role for ROCK (Bresnick, 1999; Kawano *et al*., 1999). The MLC phosphorylation state can be determined using a phospho-specific antibody that recognizes MLC only when Ser-19 is phosphorylated (Matsumura *et al*., 1998).

In agreement with findings by others (Amano *et al*., 1998), we found that differences in MLC phosphorylation on Ser-19 are hard to detect in neuroblastoma cells (our unpublished data); therefore, we turned to NIH3T3 cells. Cells were infected with control pS retrovirus (pRS) and pRS-p116Rip retrovirus (Brummelkamp *et al*., 2002b). After 3 d, cells were serum starved and then stimulated with either LPA (as a RhoA-activating agonist) or with CA, a potent inhibitor of type I phosphatases and as such a strong inducer of neurite retraction. In parallel experiments, the ROCK inhibitor Y-27632 was added to cells maintained in serum-containing medium. As shown in Figure 6, p116Rip expression levels are strongly reduced in pRS-p116Rip cells. Yet, pRS control and pRS-p116Rip cells, maintained in serum-free medium, show comparable basal levels of phosphorylated MLC (as detected by anti-phospho-MLC-Thr18/Ser19 antibody), whereas LPA and calyculin A are both capable of further enhancing MLC phosphorylation (Figure 6, bottom). Neuro-2A and N1E-115 cells underwent rapid neurite retraction and cell rounding in response to LPA and calyculin A, whereas the rounded pRS-p116Rip cells did not show any further shape change in response to either stimulus. Finally, Figure 6 shows that the ROCK inhibitor Y-27632 strongly reduces basal MLC phosphorylation in both control and p116Rip-deficient cells maintained in serum-containing medium. From these results, we conclude that p116Rip deficiency interferes with neurite outgrowth, but leaves RhoA/ROCK regulation of MLC phosphorylation intact.

Changes in p116Rip Levels Affect Detergent Solubility of MBS

Because p116Rip is an F-actin-bundling protein (Mulder *et al*., 2003), the present results suggest that p116Rip links the MBS–phosphatase complex to the cytoskeleton. To obtain biochemical evidence for this notion, we examined the association of MBS with the Triton-insoluble fraction (loosely defined as the "cytoskeletal" fraction) as a function of p116Rip expression levels. Because retroviral infections of N1E-115 and Neuro-2A were unsuccessful in our hands, we produced p116Rip RNAi-encoding adenovirus. N1E-115 cells infected with either control pAS or pAS-p116Rip adenovirus were lysed, and the solubility of MBS was determined (Mulder *et al*., 2003). As shown in Figure 7, A and B, pAS-p116Rip N1E-115 cells show complete knockdown of p116Rip, with all cells having a rounded morphology. In serum-starved control cells, MBS is ~50% insoluble in 0.1% Triton. After treatment of the cells with LPA or CA, MBS moves to the soluble fraction (Figure 7C, left), suggesting that MBS dissociates from the cytoskeleton. In p116Rip-deficient cells (serum starved), however, 80% of MBS is already found in the soluble fraction, and CA tends to shift MBS even more into the soluble fraction compared with control cells (Figure 7C, right).

Overexpression of p116Rip causes the opposite effect in that it inhibits the shift of MBS out of the pellet after treatment with LPA or CA (Figure 7D). In control experiments, we monitored the solubility of cortactin, an F-actin–binding protein that does not interact with MBS. As shown in Figure 7, C and D, cortactin moves to the insoluble fraction (in response to LPA or CA) in a manner independent of p116Rip expression levels. Note that, in growing cells, p116Rip is equally distributed between the insoluble and soluble fractions (Mulder *et al*., 2003), whereas in serum-starved cells, p116Rip is found more in the soluble fraction. Although no shift in p116Rip was detected upon LPA or CA treatment (Figure 7D, right), there is a clear correlation between the amounts of p116Rip and MBS in the insoluble fraction. It thus seems that the association of MBS with the cytoskeleton depends on p116Rip, in keeping with the notion that p116Rip functions as a scaffold that links MBS to the actin cytoskeleton.

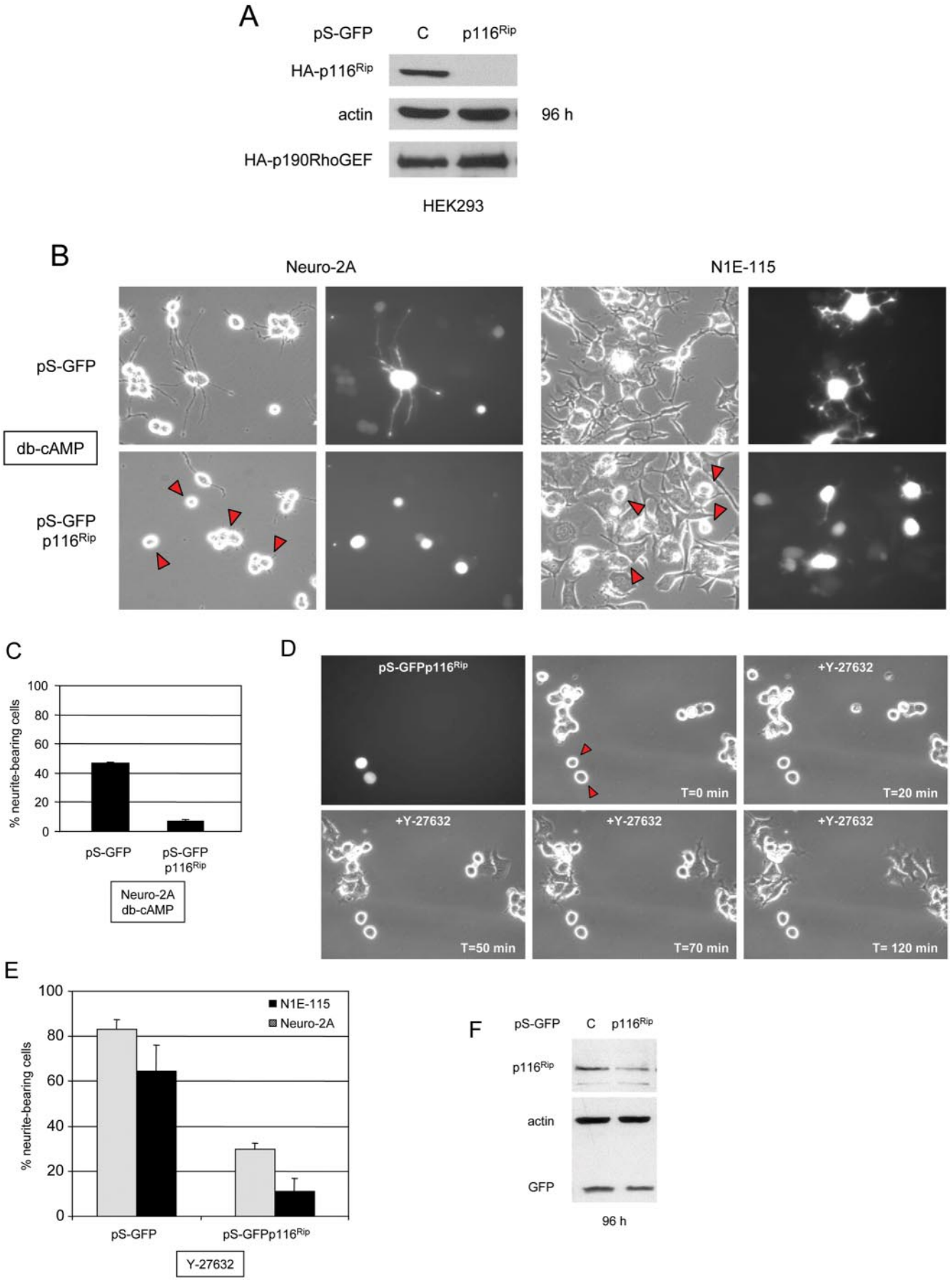
A
pS-GFP
C
p116Rip
HA-p116Rip
actin
96 h
HA-p190RhoGEF
HEK293
B
Neuro-2A
N1E-115
pS-GFP
db-cAMP
pS-GFP
p116Rip
C
% neurite-bearing cells
100
80
60
40
20
0
pS-GFP
pS-GFP
p116Rip
Neuro-2A
db-cAMP
D
pS-GFPp116Rip
T=0 min
+Y-27632
T=20 min
+Y-27632
T=50 min
+Y-27632
T=70 min
+Y-27632
T= 120 min
E
% neurite-bearing cells
100
80
60
40
20
0
N1E-115
Neuro-2A
pS-GFP
pS-GFPp116Rip
Y-27632
F
pS-GFP
C
p116Rip
p116Rip
actin
GFP
96 h

Figure 5.

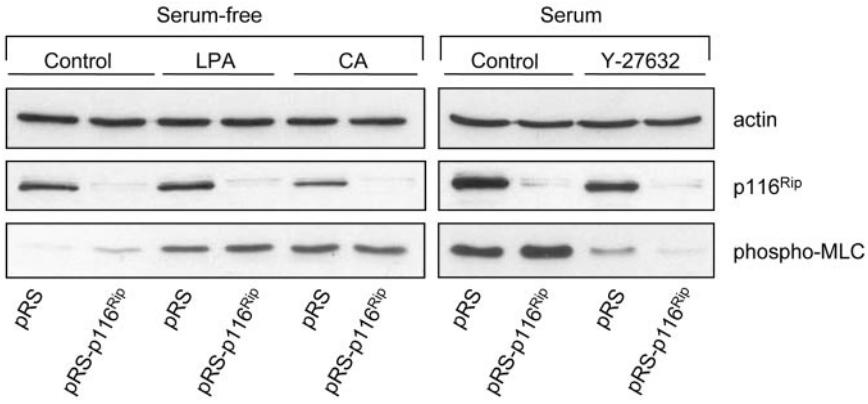

Figure 6. Knockdown of p116Rip does not affect the regulation of MLC phosphorylation. NIH3T3 cells were infected with p116Rip RNAi-encoding retrovirus (pRS-p116Rip). At 72 h after infection, cells were either serum-starved (0.1% FCS for 24 h) or left in serum-containing media. Serum-starved cells were stimulated with 2.5 μM 1-oleoyl-LPA for 10 min or with 0.1 μM CA for 5 min (left). Cells that were maintained in serum-containing medium were incubated with 10 μM Y-27632 for 45 min (right). Cells were analyzed for p116Rip expression (middle) and MLC phosphorylation (on Thr18/Ser19; bottom). Actin expression was determined to test for equal loading.

DISCUSSION

Dynamic remodeling of the actomyosin-based cytoskeleton via Rho GTPases is fundamental to neurite retraction and outgrowth, axon guidance, and dendritic branching (Luo, 2000, 2002). Mutations in components of Rho GTPase signaling pathways have been documented in human neurological disorders (for references, see Luo, 2000), which underscores the importance of Rho signaling in the development and function of the nervous system. Although many details of Rho GTPases and their regulation have been elucidated in recent years, it remains unclear how the individual components of Rho-regulated pathways are assembled into functional signaling modules and how the specificity of signal transduction is determined, although scaffold proteins are likely to play an important role.

Figure 5 (facing page). RNAi-mediated knockdown of p116Rip prevents neurite outgrowth. (A) pS-GFP (Control, C) or pS-GFPp116Rip plasmids were cotransfected with plasmids encoding HA-p116Rip or HA-p190RhoGEF (van Horck *et al*., 2001) into HEK293 cells. Cotransfection with pS-GFPp116Rip knocks down the expression of HA-p116Rip, but not the expression of HA-p190RhoGEF or actin. (B) Neuro-2A and N1E-115 neuroblastoma cells were transfected with pS-GFP or pS-GFPp116Rip plasmids. At 72 h after transfection, neurite outgrowth was induced by addition of 1 mM db-cAMP. After 2 d, cells were analyzed by fluorescence (right) and phase-contrast (left) microscopy. Arrowheads point to pS-GFPp116Rip-positive cells. (C) Neuro-2A cells were transfected with pS-GFP or pS-GFPp116Rip plasmids. At 72 h after transfection, neurite outgrowth was induced by addition of db-cAMP (1 mM). The number of GFP-positive, neurite-bearing Neuro-2A cells was determined at 48 h after addition of db-cAMP. At least 100 GFP-positive cells were counted for each experiment. Bars denote the means (±SD) of three independent experiments. (D) N1E-115 cells were transfected with pS-GFPp116Rip plasmids. At 9 h after transfection, the ROCK inhibitor Y-27632 (10 μM) was added, and subsequent changes in cell morphology were monitored by time-lapse microscopy. Note that control cells start to flatten and initiate neurite outgrowth within ~30 min of Y-27632 addition, whereas the p116Rip-deficent cells (arrowheads) fail to change their morphology. (E) As in B, the number of GFP-positive Neuro-2A or N1E-115 cells showing neurite outgrowth was determined at 8 h after addition of Y-27632 (96 h after transfection). At least 100 cells were counted for each experiment. Bars denote the means (±SD) of three independent experiments. (F) Neuro-2A cells were transfected with the indicated plasmids, lysed 96 h after transfection, and analyzed for p116Rip expression. pS-GFPp116Rip knocks down endogenous p116Rip expression, taking into account a transfection efficiency of Neuro-2A cells of ~30%.

p116Rip as a Possible Scaffold, Linking Myosin Phosphatase to F-Actin

The present study, together with our previous findings (Mulder *et al*., 2003), suggests that p116Rip serves as a scaffold that links the RhoA/ROCK-regulated myosin phosphatase complex to the F-actin cytoskeleton. p116Rip was recently characterized as an actin-binding protein that through its N-terminal domain bundles F-actin in vitro and dictates the localization of p116Rip to F-actin–rich structures, which are normally under the control of Rho GTPases, in both neuronal and nonneuronal cells (Mulder *et al*., 2003). Although p116Rip was initially isolated as a RhoA-interacting protein in a yeast two-hybrid screen (using activated V14RhoA as bait; Gebbink *et al*., 1997), our subsequent studies indicated that p116Rip is unlikely to interact directly with either RhoA-GTP or RhoA-GDP under normal physiological conditions (Gebbink *et al*., 2001; Mulder *et al*., 2003; our unpublished data). Overexpression studies showed that the N-terminal actin-binding region of p116Rip can disrupt F-actin integrity and inhibit RhoA-regulated actomoysin contractility to promote neurite outgrowth in neuroblastoma cells and process extension in NIH3T3 cells (Gebbink *et al*., 1997; Mulder *et al*., 2003). Interestingly, database analysis reveals that p116Rip is evolutionary conserved, because there are predicted orthologues in *Drosophila* and *Caenorhabditis elegans* (termed "outspread" and "F10G8.8," respectively) showing a similar domain arrangement. However, the normal function of p116Rip in cytoskeletal regulation, in general, and neuritogenesis in particular, has remained elusive.

Here, we find that the C-terminal coiled-coil domain of p116Rip interacts directly with the myosin binding subunits of MLC phosphatase MBS85 and MBS130, with selected (iso)leucine residues in the coiled-coil being essential for interaction with the C-terminal leucine zipper in MBS. Coimmunoprecipitation experiments show that the MBS130–p116Rip interaction occurs endogenously in neuronal cells (Figure 4). By modulating and targeting the catalytic phosphatase subunit (PP1δ) to the myosin II light chain, MBS130 regulates contractile processes such as neurite retraction and/or outgrowth in response to RhoA–ROCK activation. The closely related MBS85 isoform, which is highly expressed in brain and heart (but not in smooth muscle), likely acts in a very similar manner (Tan *et al*., 2001). In vivo studies on MBS85 are hampered, however, by the fact that its endogenous levels in cultured cells are much lower than those of MBS130 and antibodies are not yet available (Tan *et al*., 2001).

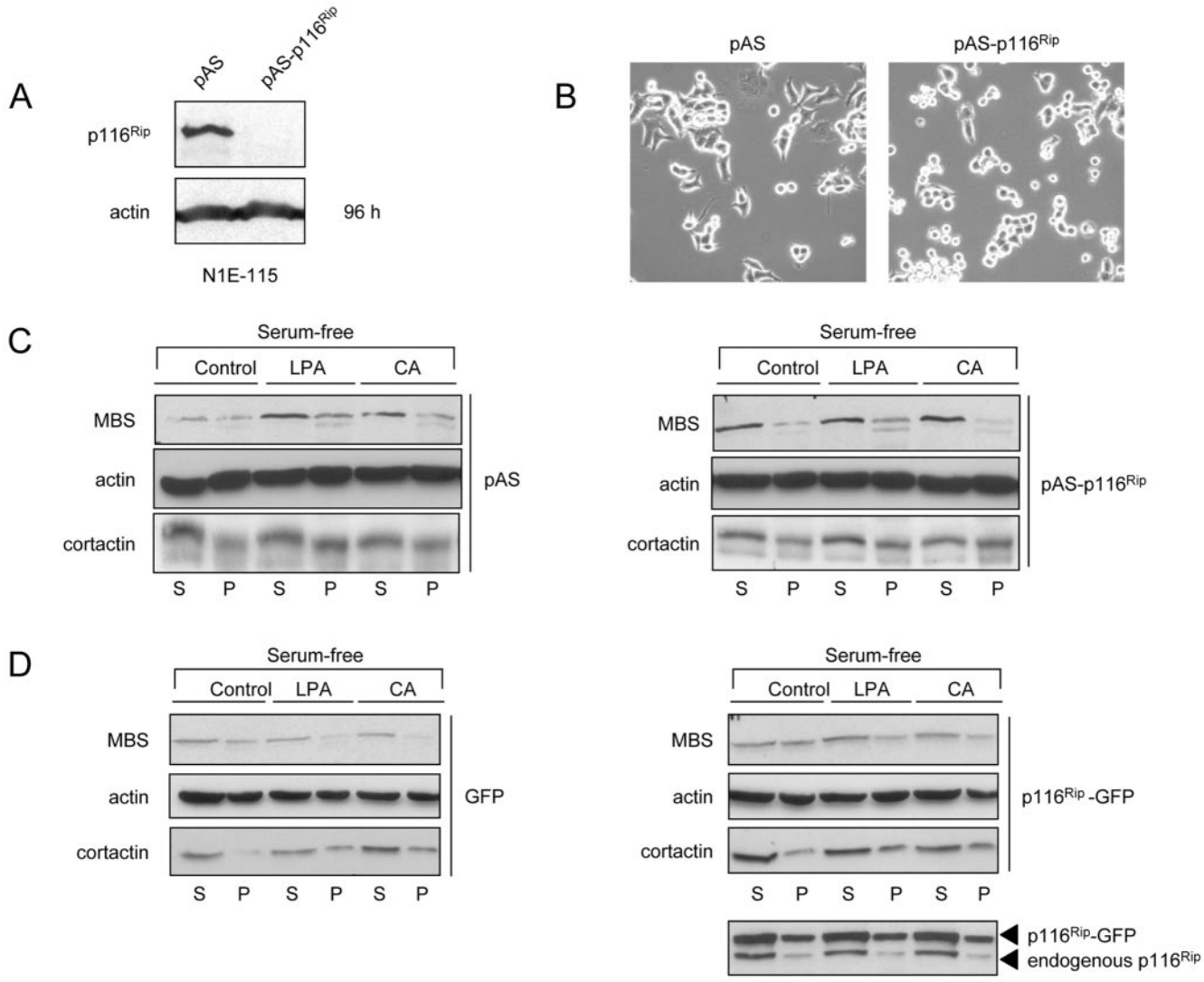

Figure 7. MBS associates with the Triton-insoluble cytoskeletal fraction in a p116^{Rip}-dependent manner. (A) N1E-115 cells were infected with control (pAS) or p116^{Rip}-RNAi-encoding (pAS-p116^{Rip}) adenovirus and lysed 96h after infection. pAS-p116^{Rip} down-regulates the expression of endogenous p116^{Rip} very efficiently. (B) N1E-115 cells were infected with control (pAS) or p116^{Rip}-RNAi-encoding (pAS-p116^{Rip}) adenovirus and viewed by phase-contrast microscopy. (C and D) At 72 h after infection, cells were serum starved. The next day, serum-starved cells were stimulated with 2.5 μM 1-oleoyl-LPA for 5 min or with 0.1 μM CA for 4 min (left). The solubility of MBS was determined using a buffer containing 0.1% Triton-X-100, and subcellular fractionation was performed resulting in a supernatant (S) and pellet (P) fraction of control pAS or pAS-p116^{Rip} infected N1E-115 cells. Supernatant and pellet fractions were immunoblotted for MBS, cortactin, and actin. (D) N1E-115 cells were transfected with GFP or p116^{Rip}-GFP constructs. Forty-eight hours after transfection, cells were serum starved overnight, stimulated, and analyzed as in C.

In addition to binding to p116^{Rip}, the C-terminal leucine zipper of MBS also interacts directly with the GTP-bound, active form of RhoA (Kimura *et al*., 1996). Binding of MBS130 to both p116^{Rip} and RhoA-GTP implies the existence of a p116^{Rip}/MBS/RhoA-GTP complex in vivo. That the interaction between p116^{Rip} and RhoA-GTP is indirect and likely very transient in nature may explain why the p116^{Rip}–RhoA association escapes detection under physiological conditions. Aside from binding to p116^{Rip} and RhoA-GTP, the leucine zipper of MBS also has been reported to bind to a 20-kDa subunit of unknown function (Hartshorne, 1998), to the ROCK-substrate moesin (at least in epithelial cells; Fukata *et al*., 1998) and to cGMP-dependent protein kinase, which mediates physiological relaxation of vascular smooth muscle (Surks *et al*., 1999). This suggests that, depending on cell type or/and its subcellular localization, MBS may exist in distinct signaling complexes with different cellular functions. In this respect, it should be noted that ROCK and the myosin phosphatase complex can regulate the phosphorylation state of proteins other than MLC (Bauman and Scott, 2002). Examples include the actin-binding proteins adducin and moesin, which interact directly with MBS and are subject to dual regulation by ROCK and MBS (Fukata *et al*., 1998; Fukata *et al*., 1999; Nakamura *et al*., 2000). It is therefore conceivable that p116^{Rip} also may be a target of myosin phosphatase. Consistent with this possibility, we find that p116^{Rip} is a phosphoprotein (Mulder, unpublished data) and associates in vivo with the whole myosin phosphatase complex, consisting of MBS and the catalytic PP1δ subunit (Figure 4B). How the phosphorylation of p116^{Rip} is regulated

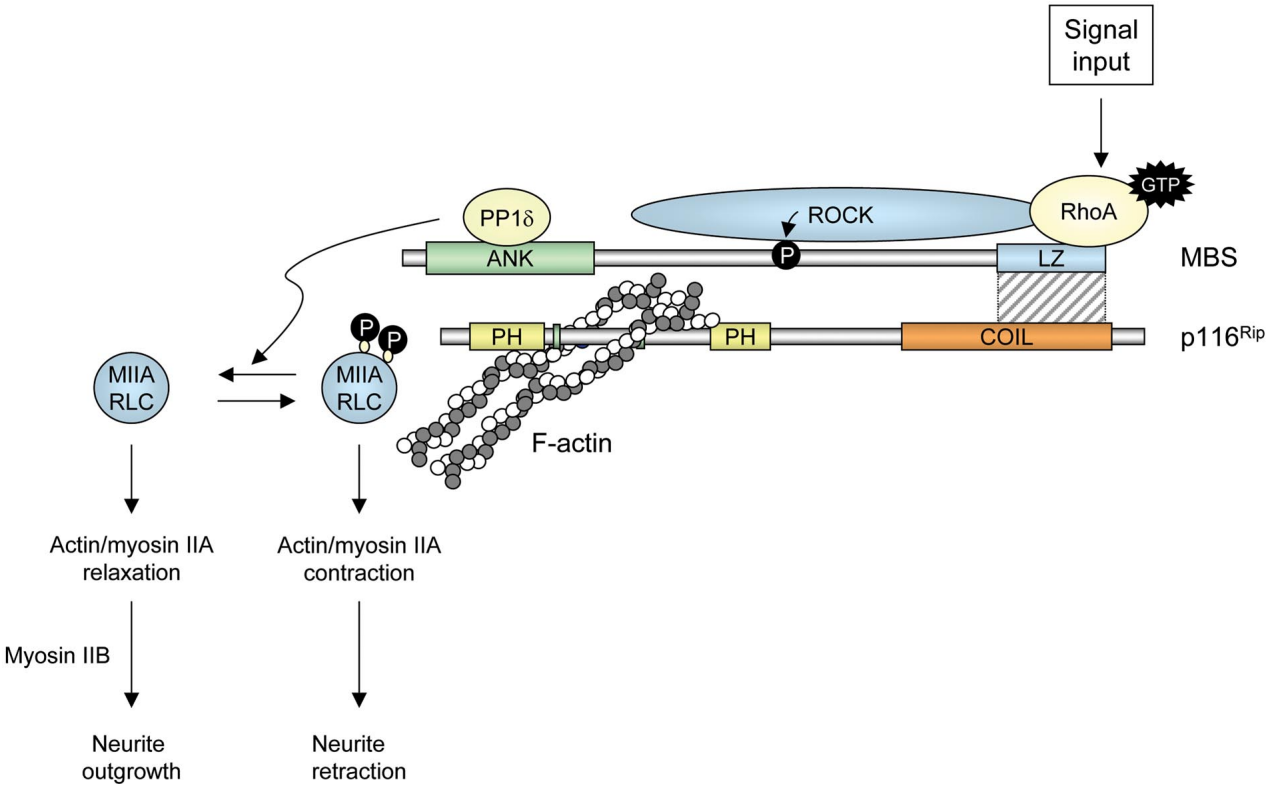

Figure 8. Model of p116Rip in association with the ROCK-regulated myosin phosphatase complex and F-actin. We propose that p116Rip acts as a scaffold whose C-terminal coiled-coil binds to the MBS subunits (MBS85 and MBS130) of nonmuscle myosin II phosphatase, whereas its N-terminal domain binds to (and bundles) F-actin (Mulder *et al.*, 2003). MBS is a direct target of ROCK and also can bind RhoA, as indicated. The location(s) of the myosin II binding sites on MBS is somewhat controversial, because binding of myosin II (or its light chain) to both N- and C-terminal regions has been reported (Hartshorne, 1998; Velasco *et al.*, 2002). MBS phosphorylation inhibits PPI activity and thereby promotes MLC phosphorylation (by one or more candidate kinases, including MLC kinase and ROCK), leading to increased myosin II activity (the conventional IIA isoform; Wylie and Chantler, 2003) and neurite retraction. Dephosphorylation of the light chain of myosin IIA may allow myosin IIB action to predominate, leading to enhanced growth cone motility and neurite outgrowth (Bridgman *et al.*, 2001; Wylie and Chantler, 2003). ANK, ankyrin repeats; LZ, leucine zipper; MIIA, myosin IIA; RLC, regulatory light chain.

and may influence its function remains a challenge for future studies.

p116Rip Is Essential for RhoA/ROCK-regulated Neuritogenesis

Knockdown studies using RNAi in Neuro-2A cells indicate that p116Rip is essential for neurite outgrowth induced by extrinsic cues that inhibit RhoA/ROCK activity, notably, 1) the RhoA-inactivating C3 exo-enzyme; 2) the ROCK inhibitor Y-27632; 3) removal of serum (a rich source of the RhoA-activating agonist LPA); and 4) treatment of the cells with db-cAMP, which raises intracellular cAMP levels to activate protein kinase A and thereby inhibits RhoA-mediated contractility at multiple levels, leading to neurite outgrowth (Dong *et al.*, 1998; Essler *et al.*, 2000; Neumann *et al.*, 2002; Snider *et al.*, 2002, and references therein). It is of note, however, that p116Rip knockdown does not interfere with MLC phosphorylation induced by either LPA or the phosphatase I inhibitor calyculin A (at least in NIH3T3 cells), nor does it inhibit Y-27632–induced MLC dephosphorylation (i.e., ROCK regulation of MLC phosphatase activity). In other words, it seems that p116Rip loss-of-function prevents ROCK from remodeling the F-actin cytoskeleton, but not from regulating MLC (de)phosphorylation. Although MLC is dephosphorylated (by Y-27632 treatment), p116Rip-deficient cells maintain their "contracted" morphology. MLC-independent regulation of contractility is, however, not without precedent (Seasholtz, 2003). Together with our previous data, the present results suggest a model in which p116Rip acts as a scaffold to link the RhoA/ROCK-regulated myosin II phosphatase complex to the actin cytoskeleton (Figure 8). As such, p116Rip is essential for actomyosin "relaxation," which is thought to be initiated by the reduced activity of the conventional myosin IIA isoform (Bridgman *et al.*, 2001; Wylie and Chantler, 2003). Reduced myosin IIA activity may allow myosin IIB action to predominate, leading to enhanced growth cone motility and neurite outgrowth (Bridgman *et al.*, 2001; Wylie and Chantler, 2003), as illustrated Figure 8.

In a recent study, the human homologue of p116Rip was identified in a yeast-two hybrid screen by using the C terminus of MBS130 as bait (Surks *et al.*, 2003). Similar to the present findings in neuronal cells, p116Rip and MBS130 were shown to interact in vascular smooth muscle cells, which led the authors to hypothesize that p116Rip serves to target RhoA to myosin phosphatase to regulate myosin phosphorylation. In this model, p116Rip would be essential for RhoA/ROCK-regulated myosin phosphorylation. Our knockdown studies show, however, that such is not the case because RNAi-induced loss of p116Rip inhibits RhoA/ROCK actomyosin activity but not the MLC (de)phophorylation machinery.

The identification of other components of the p116^{Rip} complex should provide further insight into how it participates in Rho/ROCK regulation of cytoskeletal contractility in general, and neuritogenesis in particular. Furthermore, given the importance of the RhoA–actin pathway in transcriptional regulation (Hill *et al*., 1995; Etienne-Manneville and Hall, 2002; Miralles *et al*., 2003), future studies also should examine the role of p116^{Rip} in RhoA signaling to the nucleus.

ACKNOWLEDGMENTS

We are grateful to K. Kaibuchi and T. Leung for providing plasmids and to O. Kranenburg and members of the Division of Cellular Biochemistry for helpful discussions and advice. This work was supported by the Dutch Cancer Society.

REFERENCES

Amano, M., Chihara, K., Nakamura, N., Fukata, Y., Yano, T., Shibata, M., Ikebe, M., and Kaibuchi, K. (1998). Myosin II activation promotes neurite retraction during the action of Rho and Rho-kinase. Genes Cells *3*, 177–188.

Ayscough, K.R. (1998). In vivo functions of actin-binding proteins. Curr. Opin. Cell Biol. *10*, 102–111.

Bamburg, J.R. (1999). Proteins of the ADF/cofilin family: essential regulators of actin dynamics. Annu. Rev. Cell Dev. Biol. *15*, 185–230.

Bauman, A.L., and Scott, J.D. (2002). Kinase- and phosphatase-anchoring proteins: harnessing the dynamic duo. Nat. Cell Biol. *4*, E203–E206.

Bito, H., Furuyashiki, T., Ishihara, H., Shibasaki, Y., Ohashi, K., Mizuno, K., Maekawa, M., Ishizaki, T., and Narumiya, S. (2000). A critical role for a Rho-associated kinase, p160ROCK, in determining axon outgrowth in mammalian CNS neurons. Neuron *26*, 431–441.

Borisy, G.G., and Svitkina, T.M. (2000). Actin machinery: pushing the envelope. Curr. Opin. Cell Biol. *12*, 104–112.

Bresnick, A.R. (1999). Molecular mechanisms of nonmuscle myosin-II regulation. Curr. Opin. Cell Biol. *11*, 26–33.

Bridgman, P.C., Dave, S., Asnes, C.F., Tullio, A.N., and Adelstein, R.S. (2001). Myosin IIB is required for growth cone motility. J. Neurosci. *21*, 6159–6169.

Brummelkamp, T.R., Bernards, R., and Agami, R. (2002a). A system for stable expression of short interfering RNAs in mammalian cells. Science *296*, 550–553.

Brummelkamp, T.R., Bernards, R., and Agami, R. (2002b). Stable suppression of tumorigenicity by virus-mediated RNA interference. Cancer Cell *2*, 243–247.

Da Silva, J.S., Medina, M., Zuliani, C., Di Nardo, A., Witke, W., and Dotti, C.G. (2003). RhoA/ROCK regulation of neuritogenesis via profilin IIa-mediated control of actin stability. J. Cell Biol. *162*, 1267–1279.

Dong, J.M., Leung, T., Manser, E., and Lim, L. (1998). cAMP-induced morphological changes are counteracted by the activated RhoA small GTPase and the Rho kinase ROKalpha. J. Biol. Chem. *273*, 22554–22562.

Essler, M., Staddon, J.M., Weber, P.C., and Aepfelbacher, M. (2000). Cyclic AMP blocks bacterial lipopolysaccharide-induced myosin light chain phosphorylation in endothelial cells through inhibition of Rho/Rho kinase signaling. J. Immunol. *164*, 6543–6549.

Etienne-Manneville, S., and Hall, A. (2002). Rho GTPases in cell biology. Nature *420*, 629–635.

Fukata, Y., Kimura, K., Oshiro, N., Saya, H., Matsuura, Y., and Kaibuchi, K. (1998). Association of the myosin-binding subunit of myosin phosphatase and moesin: dual regulation of moesin phosphorylation by Rho-associated kinase and myosin phosphatase. J. Cell Biol. *141*, 409–418.

Fukata, Y., Oshiro, N., and Kaibuchi, K. (1999). Activation of moesin and adducin by Rho-kinase downstream of Rho. Biophys. Chem. *82*, 139–147.

Gebbink, M.F., Kranenburg, O., Poland, M., van Horck, F.P., Houssa, B., and Moolenaar, W.H. (1997). Identification of a novel, putative Rho-specific GDP/GTP exchange factor and a RhoA-binding protein: control of neuronal morphology. J. Cell Biol. *137*, 1603–1613.

Gebbink, M.F., Kranenburg, O., Poland, M., van Horck, F.P., Houssa, B., Moolenaar, W.H. (2001). Identification of a novel, putative Rho-specific GDP/GTP exchange factor and a RhoA-binding protein: control of neuronal morphology. J. Cell Biol. *153*, 1337.

Hall, A. (1998). Rho GTPases and the actin cytoskeleton. Science *279*, 509–514.

Hartshorne, D.J. (1998). Myosin phosphatase: subunits and interactions. Acta Physiol. Scand. *164*, 483–493.

Higgs, H.N., and Pollard, T.D. (2001). Regulation of actin filament network formation through ARP2/3 complex: activation by a diverse array of proteins. Annu. Rev. Biochem. *70*, 649–676.

Hill, C.S., Wynne, J., and Treisman, R. (1995). The Rho family GTPases RhoA, Rac1, and CDC42Hs regulate transcriptional activation by SRF. Cell *81*, 1159–1170.

Hirose, M., Ishizaki, T., Watanabe, N., Uehata, M., Kranenburg, O., Moolenaar, W.H., Matsumura, F., Maekawa, M., Bito, H., and Narumiya, S. (1998). Molecular dissection of the Rho-associated protein kinase (p160ROCK)-regulated neurite remodeling in neuroblastoma N1E-115 cells. J. Cell Biol. *141*, 1625–1636.

Hu, J.C., O'Shea, E.K., Kim, P.S., and Sauer, R.T. (1990). Sequence requirements for coiled-coils: analysis with lambda repressor-GCN4 leucine zipper fusions. Science *250*, 1400–1403.

Jalink, K., van Corven, E.J., Hengeveld, T., Morii, N., Narumiya, S., and Moolenaar, W.H. (1994). Inhibition of lysophosphatidate- and thrombin-induced neurite retraction and neuronal cell rounding by ADP ribosylation of the small GTP-binding protein Rho. J. Cell Biol. *126*, 801–810.

Kaibuchi, K., Kuroda, S., and Amano, M. (1999). Regulation of the cytoskeleton and cell adhesion by the Rho family GTPases in mammalian cells. Annu. Rev. Biochem. *68*, 459–486.

Kawano, Y., Fukata, Y., Oshiro, N., Amano, M., Nakamura, T., Ito, M., Matsumura, F., Inagaki, M., and Kaibuchi, K. (1999). Phosphorylation of myosin-binding subunit (MBS) of myosin phosphatase by Rho-kinase in vivo. J. Cell Biol. *147*, 1023–1038.

Kimura, K., *et al*. (1996). Regulation of myosin phosphatase by Rho and Rho-associated kinase (Rho-kinase). Science *273*, 245–248.

Kozma, R., Sarner, S., Ahmed, S., Lim, L. (1997). Rho family GTPases and neuronal growth cone remodelling: relationship between increased complexity induced by Cdc42Hs, Rac1, and acetylcholine and collapse induced by RhoA and lysophosphatidic acid. Mol. Cell Biol. *17*, 1201–1211.

Luo, L. (2000). Rho GTPases in neuronal morphogenesis. Nat. Rev. Neurosci. *1*, 173–180.

Luo, L. (2002). Actin cytoskeleton regulation in neuronal morphogenesis and structural plasticity. Annu. Rev. Cell Dev. Biol. *18*, 601–635.

Matsumura, F., Ono, S., Yamakita, Y., Totsukawa, G., and Yamashiro, S. (1998). Specific localization of serine 19 phosphorylated myosin II during cell locomotion and mitosis of cultured cells. J. Cell Biol. *140*, 119–129.

Miralles, F., Posern, G., Zaromytidou, A.I., and Treisman, R. (2003). Actin dynamics control SRF activity by regulation of its coactivator MAL. Cell *113*, 329–342.

Mulder, J., Poland, M., Gebbink, M.F., Calafat, J., Moolenaar, W.H., and Kranenburg, O. (2003). p116Rip is a novel filamentous actin-binding protein. J. Biol. Chem. *278*, 27216–27223.

Nakamura, N., Oshiro, N., Fukata, Y., Amano, M., Fukata, M., Kuroda, S., Matsuura, Y., Leung, T., Lim, L., and Kaibuchi, K. (2000). Phosphorylation of ERM proteins at filopodia induced by Cdc42. Genes Cells *5*, 571–581.

Neumann, S., Bradke, F., Tessier-Lavigne, M., and Basbaum, A.I. (2002). Regeneration of sensory axons within the injured spinal cord induced by intraganglionic cAMP elevation. Neuron *34*, 885–893.

O'Shea, E.K., Rutkowski, R., and Kim, P.S. (1989). Evidence that the leucine zipper is a coiled coil. Science *243*, 538–542.

Postma, F.R., Jalink, K., Hengeveld, T., and Moolenaar, W.H. (1996). Sphingosine-1-phosphate rapidly induces Rho-dependent neurite retraction: action through a specific cell surface receptor. EMBO J. *15*, 2388–2392.

Seasholtz, T.M. (2003). The RHOad less traveled: the myosin phosphorylation-independent path from Rho kinase to cell contraction. Focus on "Rho kinase mediates serum-induced contraction in fibroblast fibers independent of myosin LC20 phosphorylation." Am. J. Physiol. *284*, C596–C598.

Snider, W.D., Zhou, F.Q., Zhong, J., and Markus, A. (2002). Signaling the pathway to regeneration. Neuron *35*, 13–16.

Surks, H.K., Mochizuki, N., Kasai, Y., Georgescu, S.P., Tang, K.M., Ito, M., Lincoln, T.M., and Mendelsohn, M.E. (1999). Regulation of myosin phosphatase by a specific interaction with cGMP-dependent protein kinase Ialpha. Science *286*, 1583–1587.

Surks, H.K., Richards, C.T., and Mendelsohn, M.E. (2003). Myosin phosphatase-Rho interacting protein. A new member of the myosin phosphatase complex that directly binds RhoA. J. Biol. Chem. *278*, 51484–51493.

Tan, I., Ng, C.H., Lim, L., and Leung, T. (2001). Phosphorylation of a novel myosin binding subunit of protein phosphatase 1 reveals a conserved mechanism in the regulation of actin cytoskeleton. J. Biol. Chem. *276*, 21209–21216.

Turner, R., and Tjian, R. (1989). Leucine repeats and an adjacent DNA binding domain mediate the formation of functional cFos-cJun heterodimers. Science *243*, 1689–1694.

van Ham, S.M., *et al*. (1997). HLA-DO is a negative modulator of HLA-DM-mediated MHC class II peptide loading. Curr. Biol. *7*, 950–957.

van Horck, F.P., Ahmadian, M.R., Haeusler, L.C. , Moolenaar, W.H., and Kranenburg, O. (2001). Characterization of p190RhoGEF, a RhoA-specific guanine nucleotide exchange factor that interacts with microtubules. J. Biol. Chem. *276*, 4948–4956.

Velasco, G., Armstrong, C., Morrice, N., Frame, S., and Cohen, P. (2002). Phosphorylation of the regulatory subunit of smooth muscle protein phosphatase 1M at Thr850 induces its dissociation from myosin. FEBS Lett. *527*, 101–104.

Wear, M.A., Schafer, D.A., and Cooper, J.A. (2000). Actin dynamics: assembly and disassembly of actin networks. Curr. Biol. *10*, R891–R895.

Wylie, S. R. and Chantler, P. D. (2003). Myosin IIA drives neurite retraction. Mol. Biol. Cell *14*, 4654–4666.

Zondag, G.C., Moolenaar, W.H., and Gebbink, M.F. (1996). Lack of association between receptor protein tyrosine phosphatase RPTP mu and cadherins. J. Cell Biol. *134*, 1513–1517.